Matrix Infrared Spectroscopic and ab Initio Studies of ZnH2, CdH2, and Related Metal Hydride Species

ARTICLE *in* THE JOURNAL OF PHYSICAL CHEMISTRY · MAY 1995

Impact Factor: 2.78 · DOI: 10.1021/j100020a014

Matrix Infrared Spectroscopic and ab Initio Studies of ZnH_2, CdH_2, and Related Metal Hydride Species

Tim M. Greene, Wendy Brown, Lester Andrews,* and Anthony J. Downs

Inorganic Chemistry Laboratory, University of Oxford, Oxford OX1 3QR, U.K.

George V. Chertihin

Chemistry Department, University of Virginia, Charlottesville, Virginia 22901

Nino Runeberg and Pekka Pyykkö

Department of Chemistry, University of Helsinki, PO Box 19 (Et. Hesperiankatu 4), 00014 Helsinki, Finland

Received: October 31, 1994; In Final Form: February 17, 1995[⊗]

A heated microwave discharge source of zinc and cadmium atoms and of their resonance radiation was used to form ZnH_2 and CdH_2 for infrared spectroscopic study of the matrix-isolated molecules. The reactive resonance lamp source also gives ZnH, CdH, and other related hydride species. The same hydrides have been prepared using pulsed-laser ablation of zinc and cadmium targets as the metal atom source. The ZnH_2 spectrum observed here is in agreement with that reported in earlier thermal/photolysis experiments; CdH_2 has an analogous spectrum. Coupled cluster calculations using 20-valence electron pseudopotentials give ν_2 and ν_3 values only 1−2% too high for ZnH_2, though agreement is not as good for CdH_2, with ν_2 computed 2−4% lower and ν_3 computed 2−4% higher than observed. The photosensitive dizinc species Zn_2H and Zn_2H_2 have been identified with the help of MP2 calculations and deuterium substitution.

Introduction

Although there exist several routes for the preparation of zinc and cadmium dihydrides,[1-3] these materials are associated, hydrogen-bridged polymers under normal conditions; in this respect they are similar to many main-group metal hydrides, such as BeH_2, MgH_2, and AlH_3.[4-6] To study triatomic zinc and cadmium dihydrides, it is necessary therefore to "trap" the molecules prior to the polymerization process. The technique of matrix isolation is ideally suited to allow for such physical trapping and has been employed here to generate the isolated molecule from reactions of the metal atoms with dihydrogen. Similar methods have been used recently for the synthesis and vibrational characterisation of Be, Mg, Ca, and Zn hydrides using either photochemical excitation of thermally produced atoms or pulsed-laser evaporation of metal targets.[7-10] The former method induces insertion of the metal into the H−H bond to give the dihydrides,[7,8] but the latter method provides the metal atom with sufficient kinetic energy to make both the dihydrides and the monohydrides.[9,10]

The zinc dihydride molecule has previously been isolated in an argon matrix at 12 K following the cocondensation of zinc atoms, vaporized from a resistively heated stainless steel Knudsen cell, with dihydrogen in an excess of argon.[8] No infrared features attributable to either the dihydride or the monohydride, ZnH, were observed on deposition, but subsequent photolysis with UV light yielded ZnH_2. It was decided to employ a microwave discharge to excite the metal vapor in an argon stream where the discharge provides resonance radiation to photoexcite ground-state atoms during deposition in the argon matrix. This new technique was also employed for the study of cadmium hydrides.

It has recently been suggested by Breckenridge and Wang[11] that the gas phase reaction between $Zn(^3P_1)$ and H_2 proceeds to the monohydride via the decomposition of a bent excited H−Zn−H insertion intermediate; these matrix experiments were designed to relax and trap this intermediate species.

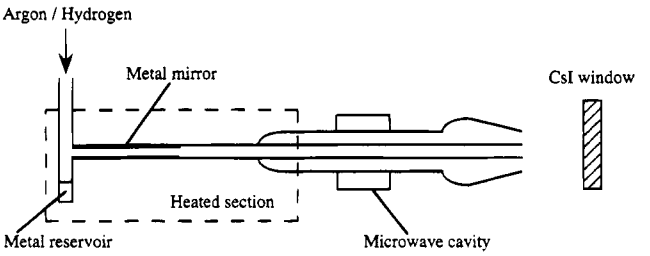

Figure 1. Schematic diagram of metal atom deposition apparatus.

Electronic and molecular structure calculations have been carried out for the ground states of the group 12 dihydrides ZnH_2,[12-16] CdH_2,[13,16] and HgH_2.[13,16-19] Vibrational frequencies are calculated here for ZnH_2, CdH_2, and HgH_2 and compared with experimental values. A calculated geometry has appeared for HZn_2H but no vibrational frequencies were given.[16] Calculated geometries and vibrational frequencies for Zn_2H, along with a few possible structures for the dimers $[ZnH]_2$ and $[ZnH_2]_2$, are also reported here.

Experimental Section

The reactive resonance lamp used for these experiments, shown in Figure 1, is essentially that employed by Brabson et al. for the study of sulfur and selenium clusters isolated in solid argon.[20] High purity zinc or cadmium as powder or wire (Aldrich) was loaded into the finger of the quartz tube and, after evacuation, was heated until a metal mirror ca. 3 cm long was obtained along a horizontal section of the tube in a region just behind the furthest extent of the discharge. Argon containing 2% H_2 was passed through the tube at a rate of approximately 3 mmol/h, and the microwave discharge was maintained at ca. 60 W while tuned for minimum reflectance (using a Microtron 200 source). The metal mirror and exposed section of the tube

[⊗] Abstract published in *Advance ACS Abstracts,* April 1, 1995.

0022-3654/95/2099-7925$09.00/0

were heated until the initial dark pink color of the discharge turned blue; this generally required a temperature in the range 200−300 °C. The gases were condensed on a CsI window cooled to ca. 12 K, with deposition generally being performed over a period of 2−3 h. The samples were subjected to subsequent broad-band photolysis using the output from an Oriel 500-W medium-pressure mercury arc with a water filter; photolysis at selective wavelengths was carried out using additional filters (Pyrex, $\lambda > 290$ nm; soda glass $\lambda > 310$ nm and a 313 nm band-pass interference filter (fwhm 16 nm), Oriel; glass $\lambda > 400$ nm). Annealing cycles with temperatures into the 15−25 K range were carried out to allow H_2 to escape from the solid argon matrix, as indicated by pressure rises inside the matrix shroud. Further annealing at temperatures up to 35−40 K allowed diffusion and reaction of trapped species.

In other respects, the experiments were carried out broadly along the lines described elsewhere.[21] An Air Products Displex CS 202 closed-cycle refrigerator gave window temperatures down to 12 K inside a shroud maintained at a pressure below 10^{-7} Torr. Temperatures were measured with a chromel vs iron-doped gold thermocouple or with a hydrogen vapor bulb. IR spectra were recorded in the range 4000−400 cm^{-1} with a Mattson Galaxy FTIR spectrometer with 0.5 cm^{-1} resolution and an accuracy of ±0.2 cm^{-1}. Argon and dihydrogen were used as supplied by BOC (Research Grade). Samples of D_2 were prepared by the action of lithium metal (BDH) on D_2O (Aldrich).

A series of complementary experiments was carried out with pulsed-laser-evaporated zinc and cadmium atoms using the apparatus and methods described earlier.[22,23] The YAG fundamental (1064 nm) at between 40 and 80 mJ/pulse was focused (10 cm focal length) onto the rotating metal target (Fisher Scientific). Metal atoms were thus co-deposited at 12 K along with 2−4% H_2, HD or D_2 (Matheson, Cambridge Isotope) in argon. Infrared spectra were recorded at 0.5 cm^{-1} resolution with a Nicolet 750 FTIR spectrometer having a MCT-B liquid nitrogen-cooled detector.

Details of Calculations

The calculations made use of the GAUSSIAN 92 package.[24] The MOLVIB 6.0 program[25] was exploited for the vibrational frequencies of the isotopically substituted species. Correlation effects were treated at the MP2 and CCSD(T) levels of theory. The heavy metals Zn,[26] Cd,[27] and Hg[27] were described using energy-adjusted 20-valence-electron (20-VE) quasirelativistic pseudopotentials (PP).

Two different basis sets were used. The first, A, has a (8s7p6d)/(311111/22111/411) basis, supplied with the PP, on the metal atom with a (4s1p)/(31/1) basis for hydrogen.[28,29] The second, more extensive basis, B, was constructed from basis A by (i) decontracting one s and one d function from the original contraction, (ii) adding one diffuse function for each symmetry, and finally (iii) adding two f functions to generate a (9s8p6d2f) basis with the (21111111/221111/31111/11) contraction scheme. The exponents of the augmented diffuse functions were selected to follow the same ratio as the two outermost exponents in the original basis set. One f function was energy optimized at the CCSD(T) level for the ^1S ground state of each metal atom. The exponent of the optimized f function ($\alpha_{f,opt}$) was then split according to 1.5 $\alpha_{f,opt}$ and 0.5 $\alpha_{f,opt}$ to give the two f functions. The basis set on hydrogen in basis B was (10s2p)/(4111111/11).[30] The exponents for the diffuse and polarization functions used in basis B are summarized in Table 1. As a technique test, the R_e and ω_e of the closed-shell diatomic species MH^+ are reported in Table 2. The results compare favorably with the large-basis, correlated values calculated by Häussermann et al.[31] At the CCSD(T)B level, both the bond lengths and the harmonic frequencies are in excellent agreement with experimental data.[32]

TABLE 1: Exponents for the Diffuse and Polarization Functions Used in Basis B

atom	α_s	α_p	α_d	α_f
Zn	0.0019	0.0146	0.0251	6.3
				2.1
Cd	0.0063	0.0126	0.0251	2.7
				0.9
Hg	0.0068	0.0129	0.0233	1.7
				0.6
H		1.39		
		0.46		

TABLE 2: Calculated Bond Lengths, R_e (pm), and Harmonic Vibrational Frequencies (cm^{-1}) for MH^+ (M = Zn, Cd, or Hg)

species	method[a]	R_e(M−H)	ω_e
ZnH^+	obs[b]	151.5	1916
	MP2A	150.2	2037
	MP2B	149.1	2014
	CCSD(T)A	152.6	1898
	CCSD(T)B	152.0	1878
CdH^+	obs[b]	166.7	1772.5
	MP2A	166.1	1838
	CCSD(T)A	168.2	1710
	CCSD(T)B	166.5	1771
HgH^+	obs[b]	159.4	2027.7
	MP2A	158.6	2066
	CCSD(T)A	159.7	1976
	CCSD(T)B	159.6	2008

[a] The suffix A(B) appended to the method label refers to basis set A(B). [b] From ref 32.

Results

Experimental results for the products of reactions of zinc and cadmium atoms with dihydrogen and the findings of the ab initio calculations will be presented in turn.

Zinc. Several experiments were carried out with Zn atoms and either a 2% H_2 in argon or 2% D_2 in argon gas mixture, with variations of the temperature of the discharge tube and of the photolysis/annealing sequence after sample deposition. Representative infrared spectra of the solid samples following deposition are shown in Figures 2a and 3a for the H_2 and D_2 reactions, respectively, and the observed infrared absorptions are listed in Table 3. The infrared spectra showed the presence of trace amounts of water, CO_2, CO, HCO, hydrocarbon, and SiO, impurities which are typical of experiments using discharge techniques.[33−40] A very weak band at 2218 cm^{-1} due to N_2O was barely detectable, a result which, along with the lack of HO_2 absorption at 1389 cm^{-1}, indicates minimal atmospheric contamination.[41,42] The major product bands at 1870.2 and 630.5 cm^{-1} agree with the previous measurements for ZnH_2 at 1870.8 and 630.9 cm^{-1}.[8] However, the ZnH_2 product was observed here on sample deposition as a result of photoexcitation from the resonance lamp source. In addition, the spectra revealed strong new bands at 1657.6 and 1493.9 cm^{-1}, the latter correlating with the 1496.5 cm^{-1} fundamental of gaseous ZnH,[32] and a sharp weak band at 1740.3 cm^{-1}. Analogous bands were observed in the D_2 spectrum, as listed in Table 3. The lower frequency ZnD_2 band was observed here at 454.4 cm^{-1}, near the 453.7 cm^{-1} estimate made by the Rice group.[8] It is noteworthy that the absorption due to the antisymmetric stretching mode of ZnD_2 showed partially resolved fine structure for the three major zinc isotopes; the natural isotopic components

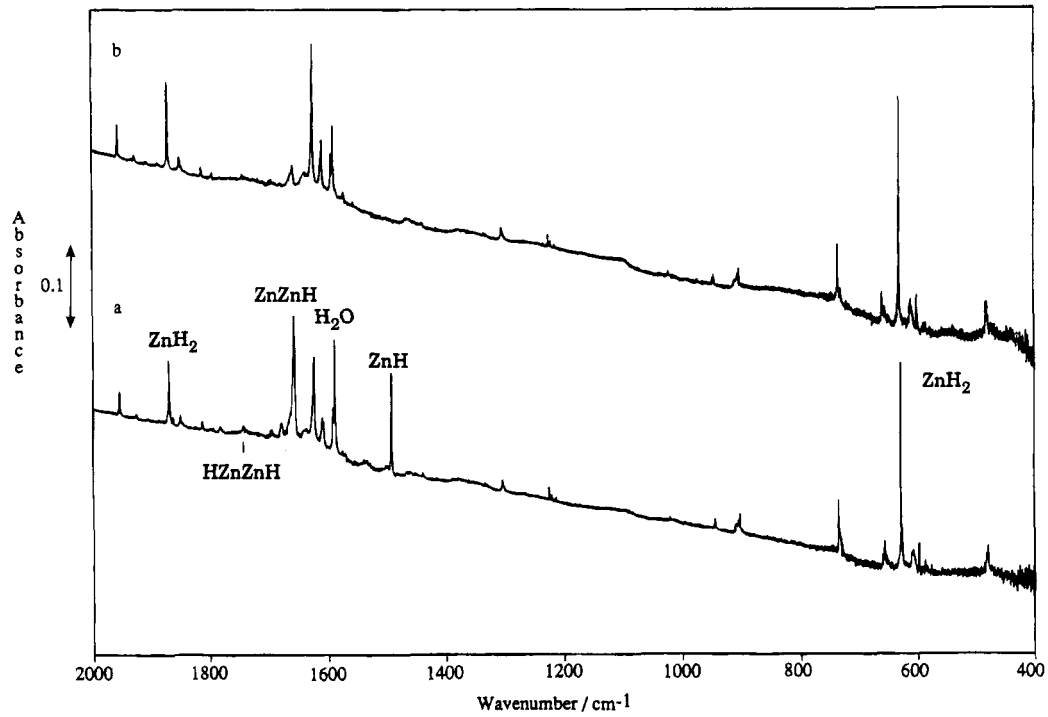

Figure 2. (a) Infrared spectrum of the deposit formed by cocondensing zinc, H_2 and argon at 12 K and (b) infrared spectrum after broad-band photolysis of the deposit.

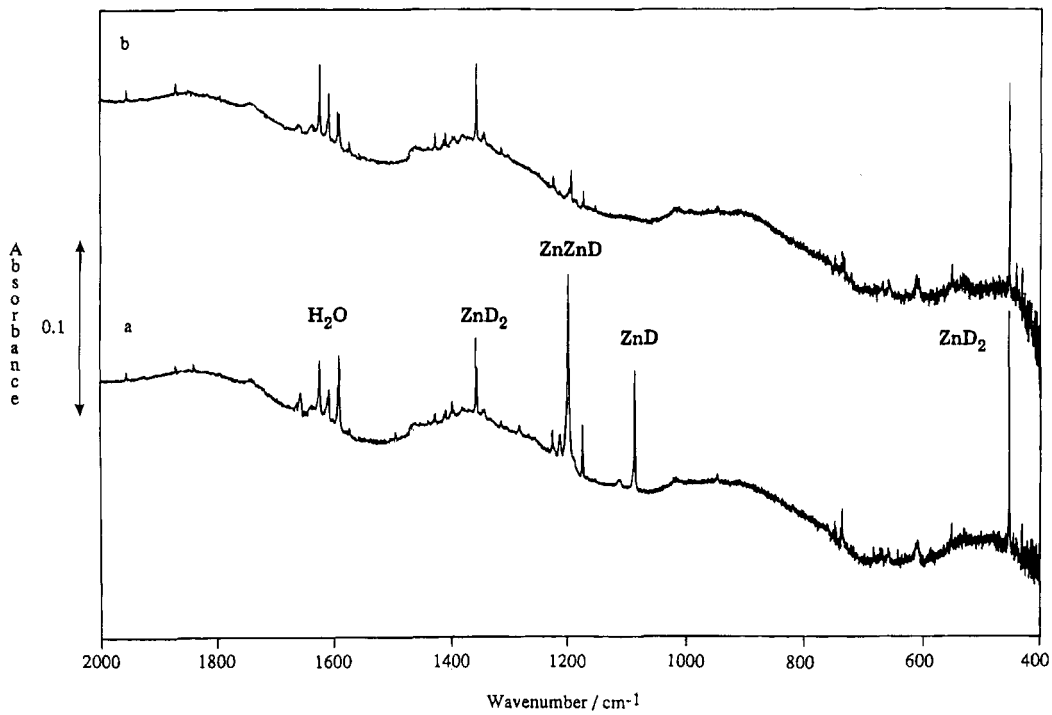

Figure 3. (a) Infrared spectrum of the deposit formed by cocondensing zinc, D_2 and argon at 12 K and (b) infrared spectrum after broad-band photolysis of the deposit.

appeared at 1357.2 ($^{64}ZnD_2$), 1356.2 ($^{66}ZnD_2$), and 1355.0 cm^{-1} ($^{68}ZnD_2$).

An experiment was carried out in which the zinc mirror was allowed to remain at room temperature so that only very small quantities of zinc were evaporated into the discharge region. Even with the lower zinc concentration, the ZnH_2 and ZnH bands were observed with relatively high intensities, but the bands at 1657.6 and 1740.3 cm^{-1} were absent. When the zinc reservoir was heated to the highest temperature, the increased zinc concentration favored the buildup of the band at 1657.6 cm^{-1}.

A final experiment was carried out in which Ar/Zn from the discharge was codeposited with a separate Ar/H_2 sample. The bands at 1870.2 and 630.5 cm^{-1} were increased while those at 1493.9 and 1657.6 cm^{-1} were reduced in intensity, relative to the spectrum shown in Figure 2a, where H_2 was discharged with Zn in the argon stream.

Zinc atoms may also form complexes with water molecules present as an impurity. Such complexes have been studied by Kauffman et al.,[43] and weak features observed at 1587.4 and 1585.3 cm^{-1} in both the hydrogen and deuterium experiments are in agreement with those previously identified with species

TABLE 3: Infrared Absorption Frequencies (cm^{-1}) Observed following the Deposition of Argon/Zinc/Hydrogen or Argon/Zinc/Deuterium Mixtures at 12 K

Zn/H_2	Zn/D_2[a]		p/a[b]	identity[c]
1955.0	1955.0	1410.0	+/−	HZnOH
1927.1				common to Cd
1870.2	1869.7, 1345.6	1357.2	+/−	ZnH_2
1849.2		1343.2	+/+	(H_2··ZnH_2)
1824.4		1331.6	−/+	(X··ZnH_2)
1812.3		1315.0		common to Cd
1782.2		1284.4	−/0	(ZnH^+)
1740.3		1254.9	−/+	HZnZnH
1667.5		1204.6		ZnZnH
1657.6	1657.6	1198.6	−/+	ZnZnH
1624.0	1427.1	1194.7		
1610.1	1413.4	1188.8		H_2O
1589.3	1398.7	1174.2		H_2O
1587.4		1587.4	−/+	(H_2O··Zn)
1585.3		1585.3		(H_2O··Zn)
1540			−/−	X··ZnH
1530.5		1111.1	−/+	H_2··ZnH
1493.9	1493.9	1087.5	−/−	ZnH
1304.9		1304.9		CH_4
1225.6		1225.6		SiO
1221.7		1221.6		SiO
1214.7		1214.7		SiO
947.1		947.1		C_2H_4
905.0		905.0		common to Cd
736.5		736.5		C_2H_2
660.0		660.0	+/−	HZnOH
649.9			+/−	ZnOH
630.5	553.0	454.4	+/−	ZnH_2
610		612	+/−	*d*
600.0		431.7	+/+	(H_2··ZnH_2)
578.8		416.2	−/+	(X··ZnH_2)
481.4			+/−	HZnOH

[a] First column lists bands due to H-containing products (from traces of HD in the D_2); second column lists bands due to products containing exclusively D. [b] Effects of photolysis (p)/annealing (a); bands unchanged (0), increase (+), or decrease (−). [c] Entries in parentheses represent tentative assignments. [d] Broad band due to unknown species.

such as H_2O··Zn. Furthermore, photochemical reaction of atomic Zn with a water molecule is reported to generate ZnOH, the Zn−O stretching frequency of which we observe at 649.9 cm^{-1}, again in agreement with earlier results.[43]

Broad-band photolysis had a dramatic effect on the infrared spectra, as shown in Figures 2b and 3b. The absorptions due to ZnH_2 increased, as expected on the basis of the earlier experiments showing the photochemical formation of ZnH_2,[8] while the absorptions due to ZnH, the strong 1657.6 cm^{-1} band and the weak 1740.3 cm^{-1} band decreased markedly on photolysis. Several weaker product bands increased or decreased as noted in Table 3. The effect of broad-band photolysis on the sample prepared by codeposition was essentially identical. To determine the radiation reponsible for the photochemistry, long-wavelength pass filters were employed. In two studies, it was found that radiation of $\lambda > 400$ nm had no effect on the infrared spectrum of the deposit, while light transmitted by the Pyrex filter ($\lambda > 290$ nm) had the same effect as did broad-band photolysis. In one experiment, radiation of $\lambda > 310$ nm destroyed the bands at 1657.6 and 1493.9 cm^{-1} with a small increase in the features at 1870.2 and 630.5 cm^{-1}. Subsequent photolysis with $\lambda > 290$ nm caused an additional increase in the intensity of the latter two bands.

Annealing caused a decrease in the intensity of most of the bands listed in Table 3 except those at 1849.2, 1740.3, 1657.6, and 600.0 cm^{-1} which increased. Upon final annealing to 35−38 K, a new set of bands appeared at 1824.4, 1667.5, 1530.5, and 578.8 cm^{-1}.

TABLE 4: Frequencies (cm^{-1}) of New Infrared Absorptions Observed Following the Deposition of Argon/Cadmium/ Hydrogen or Argon/Cadmium/Deuterium Mixtures at 12 K

Cd/H_2	$Cd/H_2/D_2$	Cd/D_2	p/a[a]	identity[b]
1836.9	1836.9, 1319.8	1836.9, 1319.8	+/0	HCdOH
1753.5	1756.2, 1260.3	1756.2, 1264.4	+/−	CdH_2
1718.6		1239.6	+/+	(H_2··CdH_2)
1580.7		1168.4	−/+	H_2O··Cd
1572.4		1161.5	−/+	H_2O··Cd
1521.0	1521.0, 1098.0	1098.0	−/+	CdCdH
1379.6		1003.3	−/−	(X··CdH)
1372.9		995.6	−/+	H_2··CdH
1339.4	1339.4, 974.4	974.4	−/−	CdH
604.6	529.9	434.2	+/−	CdH_2
601.7	527.5	432.5	+/−	CdH_2
586.7			+/+	(H_2··CdH_2)

[a] Effects of photolysis (p)/annealing (a): bands unchanged (0), increase (+), or decrease (−). [b] Entries in parentheses represent tentative assignments.

To complement the experiments with the discharge metal atom source, pulsed-laser-evaporated Zn atoms were allowed to react with H_2 in a condensing argon stream. A definite laser power threshold was observed for these metal reactions. For Zn a 40 mJ/pulse laser power at the sample gave a weak 1870.6 cm^{-1} band, but doubling the laser power intensified the 1870.6 cm^{-1} band by an order of magnitude. Results for Zn are summarized in Figure 4. The same major absorptions at 1870.6, 1657.9, 1493.9, and 630.5 cm^{-1} were observed for the reaction with H_2, along with a very weak, sharp band at 1740.3 cm^{-1}. Stepwise annealing from 12 to 50 K in 5−10 K intervals caused a gradual decrease of the 1493.9 cm^{-1} band, a sharpening and slight increase of the band at 1870.6 cm^{-1}, along with the appearance of a new satellite at 1667.9 cm^{-1}, and a 4-fold growth of the weak, sharp band at 1740.3 cm^{-1}. The spectrum after annealing to 40 K is shown, along with the deposition spectrum of the $Zn/H_2/Ar$ sample, in Figure 4a. The analogous spectrum for the D_2 reaction is illustrated in Figure 4c; noteworthy are the strong deuterium product bands at 1357.5 cm^{-1}, which shows zinc isotope splitting, 1199.0, 1087.5, and 454.2 cm^{-1} and the sharp, weak 1254.9 cm^{-1} band, which grew markedly on annealing. Of particular importance is the comparison that may be drawn with the spectrum of the HD reaction products shown in Figure 4b. First, the sharp ZnH and ZnD absorptions and the broader bands at 1657.9 and 1199.0 cm^{-1} were observed to be unshifted. Second, the same bands were observed at 1357.5, 630.5, and 454.2 cm^{-1} but with reduced intensity, along with new bands at 1870.4, 1346.2, and 553.4 cm^{-1}. Third, the same sharp, weak bands appeared at 1740.3 and 1254.9 cm^{-1} on annealing but were now accompanied by new bands of comparable intensity at 1756.4 and 1267.1 cm^{-1}. Fourth, sharp satellite features were observed at 528.9 and 511.1 cm^{-1} beside the 533.4 cm^{-1} band.

Cadmium. Similar discharge tube experiments were also carried out using cadmium as the metal reactant. The Cd/H_2 system gave on deposition a spectrum (Figure 5a) dominated by strong, sharp bands at 1753.5 and 1339.4 cm^{-1}, together with a doublet at 604.6/601.7 cm^{-1}. Weaker features at 1836.9 and 1718.6 cm^{-1} appeared to have counterparts in the Zn/H_2 system. Table 4 lists the observed frequencies of bands displayed by the Cd/H_2 system which had not previously been observed in the experiments with the Zn/H_2 system, and may therefore be inferred to arise from reaction products containing Cd. Annealing cycles to temperatures in the 35−40 K range resulted in the growth of the bands at 1718.6, 1580.7, 1372.9, and 586.7 cm^{-1} but had little effect on the other features. Subsequent broad-band photolysis for 2 h caused a decrease in the intensity of the band at 1580.7 cm^{-1}, while destroying the

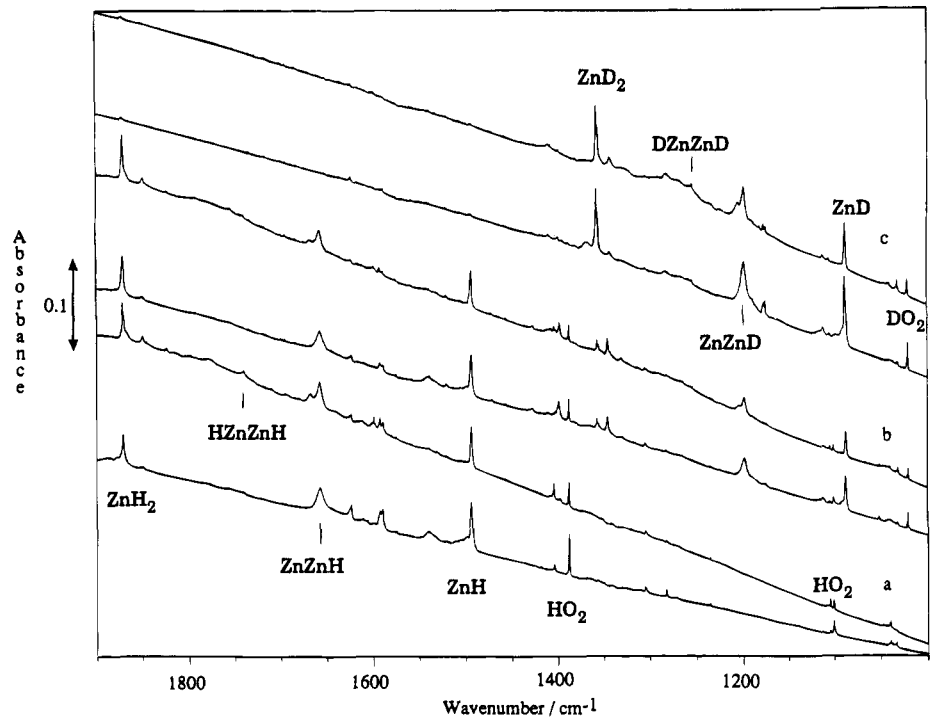

Figure 4. Infrared spectra of argon matrices including pulsed-laser evaporated Zn atoms and H_2 after condensation at 12 K. (a) 2% H_2 (bottom) and after a 12−40−12 K annealing cycle (top); (b) 4% HD and after a 12−40−12 K annealing cycle; and (c) 4% D_2 and after a 12−40−12 K annealing cycle.

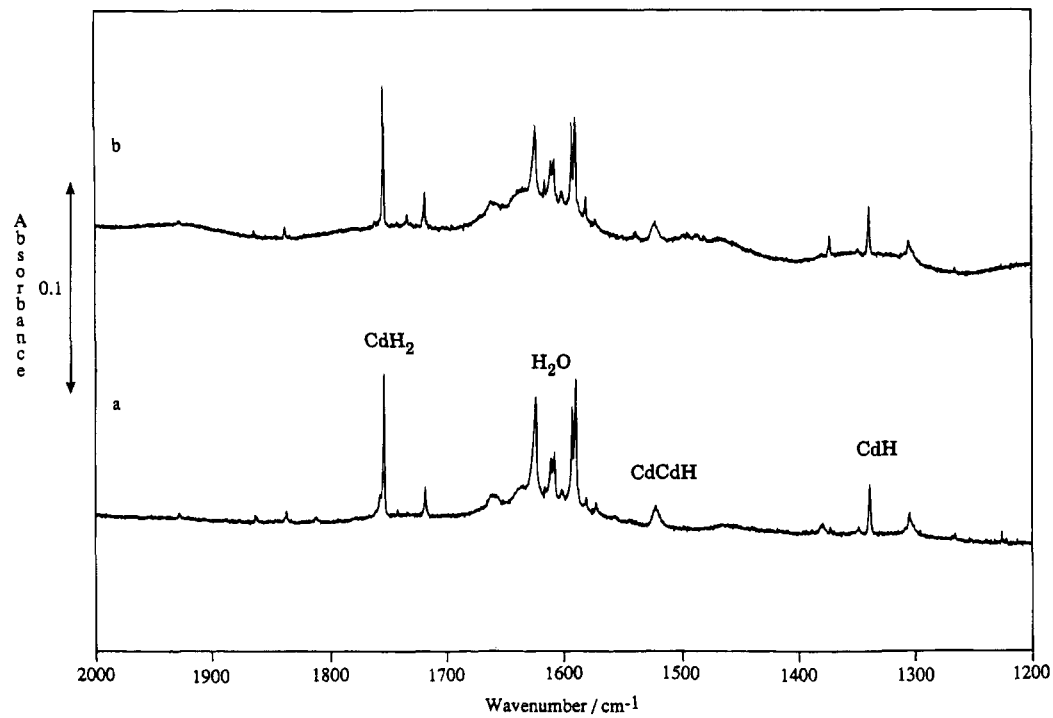

Figure 5. (a) Infrared spectrum of the deposit formed by co-condensing cadmium, H_2, and argon at 12 K and (b) infrared spectrum of the same deposit after annealing.

features at 1521.8, 1379.6, 1372.9, and 1339.4 cm^{-1}. A slight growth of the band at 1753.5 cm^{-1} and of the doublet at 604.6/601.7 cm^{-1} was observed, while the 1836.9 cm^{-1} band doubled in intensity. In another Cd/H_2 experiment, photolysis before annealing caused a marked enhancement of the group of absorptions at 1753.5 and 604.6/601.7 cm^{-1}. In a final experiment, irradiation through a 313 nm interference filter backed by Pyrex doubled the intensity of the bands at 1753.5 and 604.6/601.7 cm^{-1}, while subsequent photolysis with $\lambda >$ 310 nm destroyed the band at 1339.4 cm^{-1} and slightly increased the 1753.5, 604.6/601.7 cm^{-1} bands; photolysis with $\lambda >$ 290 nm provided more growth of this latter set of bands.

Cadmium experiments were also carried out using D_2 and H_2/D_2 mixtures. The infrared spectra of the matrices following photolysis are contrasted in Figure 6. On deposition, the strongest bands in the D_2 system appeared at 1264.4, 974.4, and 434.2/432.5 cm^{-1}. The feature at 974.4 cm^{-1} was destroyed by broad-band and Pyrex-filtered photolysis, whereas the other bands were observed to increase 3−4 fold. In the mixed H_2/D_2 system (H_2:D_2 = ca. 1:1), strong, equally intense bands at

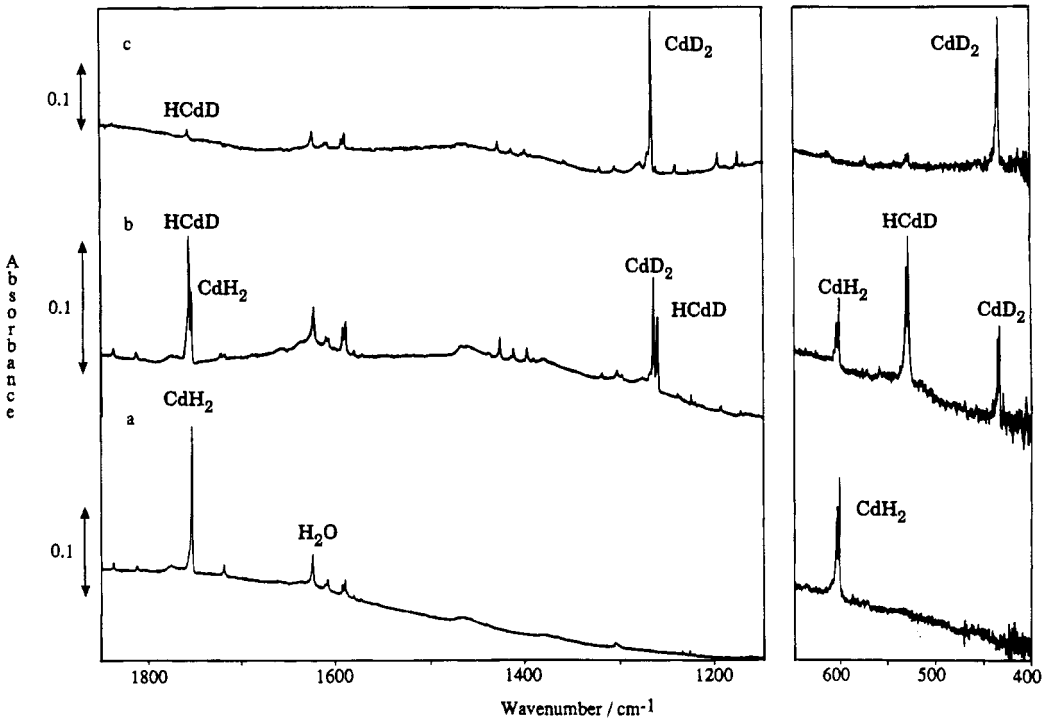

Figure 6. Infrared spectra of argon matrices following broad-band photolysis: (a) matrix containing Cd and D_2; (b) matrix containing Cd and H_2 + D_2; and (c) matrix containing Cd and H_2.

1339.4 and 974.4 cm^{-1} were both destroyed by photolysis. In addition to the growth of product bands which had been observed in the H_2 and D_2 systems individually, there appeared a new set of infrared features at 1756.2, 1260.3, 529.9, and 527.5 cm^{-1} which grew on photolysis. Deuterium counterparts of weaker product bands are listed in Table 4.

Cadmium experiments with the pulsed-laser source gave analogous spectra. The major bands were observed in H_2 and D_2 pulsed-laser Cd experiments within 0.5 cm^{-1} of those reported above (Table 5). Experiments using HD showed infrared features at 1521.0, 1339.4, and 974.4 cm^{-1} to be unshifted, while weak bands appeared at 1754.0 (shoulder), 1264.8 and 601.7 cm^{-1}. Strong new absorptions found at 1756.9, 1260.8, and 527.4 cm^{-1} decreased subsequently under the action of stepwise annealing.

Calculations. The calculated bond lengths and vibrational frequencies of the species MH_2, MHD, and MD_2 (M = Zn, Cd, or Hg) are given in Table 5. The vibrational frequencies computed for ZnH_2 and CdH_2 lend strong support to our interpretation of the matrix experiments. Moreover, the present results for HgH_2 are in good agreement not only with the QCISD(T) calculations by Schwerdtfeger et al.[18] but also with the experimentally observed vibrational frequencies.[44] The Hg−H bond is predicted to be shorter than the Cd−H bond, in keeping with the results of previous calculations.[13] The overall reactions to form the dihydride molecule from ground state metal atoms and dihydrogen are *endothermic* by 0.33, 0.74, and 1.05 eV for Zn, Cd and Hg, respectively, at the CCSD(T)B level. Table 6 summarizes the calculated energies.

The zinc monohydride, ZnH, has been studied at high levels of theory.[45,46] The present MP2B calculated frequency, 1705 cm^{-1}, compares favorably with estimates based on higher level calculations. The linear dizinc monohydride, Zn_2H, was also explored at the MP2B level; frequencies are listed in Table 7, and the structure is given in Figure 7. Similar calculations carried out for the Zn_2H^+ cation gave shorter bonds (245.5 and 148.9 pm) and higher frequencies (198, 315, and 2062 cm^{-1}).

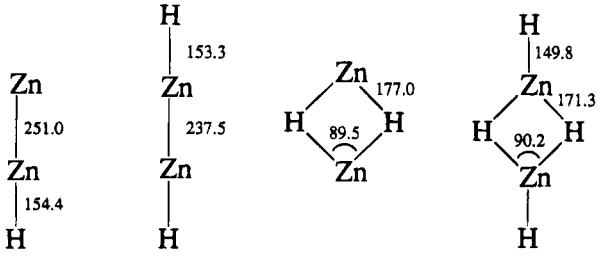

Figure 7. Optimized structures calculated at the MP2 level (basis set B) for linear Zn_2H, the linear ($D_{\infty h}$) and rhombic (D_{2h}) $[ZnH]_2$ dimers, and the $[ZnH_2]_2$ dimer (D_{2h}). Distances given in picometers, angles in degrees.

Among the possible dimers of ZnH, both the linear ($D_{\infty h}$) and the rhombic (D_{2h}) structures have been considered. The MP2B optimized geometries are shown in Figure 7, and the calculated frequencies for the linear and the rhombic structures are given in Tables 8 and 9, respectively. At the MP2B level, the dimerization energy for the linear structure was found to be −2.58 eV, compared to −1.29 eV for the rhombic structure. The BSSE-error in the dimerization energy of the linear structure was estimated by a counterpoise correction to be less than 0.1 eV.

The MP2B optimized structure of the ZnH_2 dimer (D_{2h}) is also shown in Figure 6 and the corresponding vibrational frequencies are given in Table 10. The hydrogen-bridged structures of this and of the rhombic ZnH dimer may well provide a guide to the forms adopted by polymeric zinc hydride species at normal temperatures, although no infrared bands attributable to $[ZnH_2]_2$ were observed in the matrix experiments described here.

Discussion

Several simple metal and dimetal hydride products will be identified and the mechanisms of formation discussed.

MH_2. The strong bands at 1870.2 and 630.5 cm^{-1} are assigned, respectively, to ν_3 and ν_2 of ZnH_2 on the basis (i) of

TABLE 5: Calculated Bond Lengths, R_e (in pm), and Vibrational Frequencies (in cm^{-1}) for MH_2 Molecules (M = Zn, Cd, or Hg)

species	method[a]	R_e(M−H)	ν_1 (σ_g)	ν_2 (π_u)	ν_3 (σ_u)
HZnH	obs[b]		IR-inactive	630.5	1870.6
	MP2A	151.1	2031	678	2039
	MP2B	150.5	2021	684	2001
	CCSD(T)A	153.0	1939	631	1955
	CCSD(T)B	152.7	1926	637	1921
HZnD	obs[b]		1346.2	553.4	1870.4
	MP2A		1451	590	2035
	CCSD(T)A		1388	549	1947
	CCSD(T)B		1371	555	1923
DZnD	obs[b]		IR-inactive	454.2	1357.5
	MP2A		1437	487	1464
	CCSD(T)A		1372	453	1404
	CCSD(T)B		1362	458	1379
HCdH	obs[b]		IR-inactive	601.7	1753.8
	MP2A	167.2	1858	606	1844
	CCSD(T)A	168.3	1794	574	1790
	CCSD(T)B	166.8	1850	593	1829
HCdD	obs[b]		1260.8	527.4	1756.9
	MP2A		1315	527	1851
	CCSD(T)A		1273	499	1792
	CCSD(T)B		1307	515	1839
DCdD	obs[b]		IR-inactive	432.5	1264.9
	MP2A		1314	433	1316
	CCSD(T)A		1269	410	1278
	CCSD(T)B		1309	423	1305
HHgH	obs[c]		IR-inactive	773	1896
	QCISD(T)[d]	164.1			1988
	MP2A	163.0	2134	777	1990
	CCSD(T)A	164.2	2044	749	1920
	CCSD(T)B	163.9	2082	802	1960
HHgD	obs[c]		1392	674	1946
	MP2A		1456	674	2068
	CCSD(T)A		1401	650	1987
	CCSD(T)B		1429	696	2025
DHgD	obs[c]		IR-inactive	555	1365
	MP2A		1510	553	1414
	CCSD(T)A		1446	532	1365
	CCSD(T)B		1473	570	1393

[a] The suffix A(B) appended to the method label refers to basis A(B). [b] Values taken from pulsed-laser experiments for a consistent H_2, HD, D_2 data set. [c] From ref 44. [d] From ref 18.

TABLE 6: Calculated Energies (au) for Zn, Cd, Hg, H_2, and the Metal Dihydride Molecules (Heat of Formation (eV) for $M + H_2 \rightarrow MH_2$)

system	MP2A	CCSD(T)A	CCSD(T)B
Zn	−226.318 62	−226.299 76	−226.717 08
Cd	−166.968 81	−166.985 28	−167.434 27
Hg	−152.681 38	−152.698 25	−153.120 14
H_2	−1.155 45	−1.163 72	−1.171 74
ZnH_2	−227.471 62	−227.453 29	−227.876 78
CdH_2	−168.104 16	−168.124 17	−168.578 86
HgH_2	−153.811 26	−153.831 38	−154.253 39
$Zn + H_2 \rightarrow ZnH_2$	0.067	0.277	0.328
$Cd + H_2 \rightarrow CdH_2$	0.547	0.676	0.739
$Hg + H_2 \rightarrow HgH_2$	0.696	0.833	1.048

TABLE 7: Calculated Vibrational Frequencies (in cm^{-1}) for the Linear Zn_2H Molecule ($C_{\infty v}$)[a]

	σ	π	σ
Zn_2H	175	263	1830
Zn_2D	174	190	1305

[a] Calculated for the optimized geometry (Figure 7) at the MP2B level.

the H/D ratios (1.3780 and 1.3875, respectively), (ii) of the observation of bands at 1870.6, 1346.2, and 553.4 cm^{-1} for HZnD (Table 5), and (iii) of the agreement between previous thermal evaporation/photolysis experiments[8] and the present studies employing a microwave discharge or pulsed-laser atom source of the metal. The partially resolved fine structure displayed by the ν_3 band of ZnD_2 and attributable to the major zinc isotopes verifies the vibration of a single metal atom.

TABLE 8: Calculated Vibrational Frequencies (in cm^{-1}) for the Linear HZnZnH Molecule ($D_{\infty h}$)[a]

	σ_g	π_u	π_g	σ_u	σ_g
HZnZnH	252	353	452	1884	1919
HZnZnD	251	276	418	1355	1902
DZnZnD	250	252	331	1343	1368

[a] Calculated for the optimized geometry (Figure 7) at the MP2B level.

TABLE 9: Calculated Vibrational Frequencies (in cm^{-1}) for the Rhombic $[ZnH]_2$ Molecule (D_{2h})[a]

a_g	b_{1u}	b_{3u}	b_{3g}	b_{2u}	a_g
220	466	708	931	1173	1481

a Calculated for the optimized geometry (Figure 7) at the MP2B level.

TABLE 10: Calculated Vibrational Frequencies (in cm^{-1}) for the Dimeric $[ZnH_2]_2$ Molecule (D_{2h})[a]

b_{3g}	a_g	b_{3u}	b_{2g}	b_{2u}	b_{3u}	b_{1u}	b_{3g}	b_{2u}	a_g	b_{1u}	a_g
179	251	302	444	509	750	1223	1243	1249	1575	2026	2037

[a] Calculated for the optimized geometry (Figure 7) at the MP2B level.

The strong band at 1753.5 cm^{-1} and the doublet at 604.6/601.7 cm^{-1} in the Cd experiments exhibit behavior similar to that of the bands associated with ZnH_2 and are assigned to ν_3 and ν_2 of CdH_2 on the basis (i) of the H/D ratios (1.3868 and 1.3924/1.3912, respectively) and (ii) of the observation of bands for the mixed isotopic species, HCdD, as given in Tables 4 and 5. Finally, similar discharge experiments performed with Hg gave sharp HgH_2 bands at 1895.3 and 772.9 cm^{-1} in agreement with KrF laser photolysis studies[44] and so lends support to the present identification of ZnH_2 and CdH_2.

The vibrational assignments to matrix-isolated ZnH_2 and CdH_2 are strongly supported by the quantum chemical calculations, as shown in Table 5. It is noteworthy that the larger basis set, B, gave better calculated values for ν_3, the antisymmetric stretching mode of ZnH_2, but poorer values for ν_2, the bending mode, while the reverse was true for CdH_2. As expected, the coupled cluster level of electron correlation gave more realistic frequencies than second order Moeller−Plesset theory for ZnH_2 and CdH_2. The coupled cluster calculations gave ν_3 values 2.7−4.5% too high and ν_2 values 0−1.0% too high for ZnH_2, and ν_3 values 2.1−4.3% too high and ν_2 values 1.4−4.6% too low for CdH_2. Clearly, some of this discrepancy is due to the comparison of calculated harmonic frequencies with observed anharmonic values. In this connection, it may be remarked that the ZnH_2/ZnD_2 ratios for ν_3 (1.3780) and ν_2 (1.3875) and the CdH_2/CdD_2 ratios for ν_3 (1.3868) and ν_2 (1.3924/1.3912) indicate significantly different anharmonicity terms for the ν_3 and ν_2 modes.

It is clear from the experiments carried out by Xiao et al.[8] that atomic zinc in its electronic ground state does not react with molecular hydrogen, since no products were observed on deposition. This can be explained using simple MO considerations. When zinc interacts with molecular hydrogen in C_{2v} symmetry, the 4s orbital of the metal center and the σ_g orbital of H_2 combine to form a bonding and antibonding molecular orbital, both of which are fully occupied, and so no net bonding interaction results. Thus it may be concluded that it is necessary to promote one of the 4s electrons of zinc, i.e. $4s^14p^1 \leftarrow 4s^2$

in order to induce insertion of the metal atom into the H−H bond. Two transitions are possible, namely, $^3P_1 \leftarrow {}^1S_0$, which is reported at 295 and 298 nm in an argon matrix, and $^1P_1 \leftarrow {}^1S_0$ at 207 nm in the same matrix.[47] The corresponding transitions for cadmium have also been measured previously. Cadmium atoms isolated in an argon matrix show a strong Cd $^1P_1 \leftarrow {}^1S_0$ transition at 220 nm and a much weaker Cd $^3P_1 \leftarrow {}^1S_0$ transition consisting of an asymmetric doublet at 313 and 311 nm.[47]

The zinc and cadmium dihydrides are formed on codeposition using the discharge resonance lamp and on Pyrex-filtered photolysis of the cold sample. The matrix filtered-photolysis studies with Mg[7] and recent half-collision studies with Cd[48] show that the $^1P_1$ atomic state reacts efficiently with hydrogen, and some of the metal dihydride we observe on sample deposition could arise from the $^1P_1$ photochemical reaction. However, the Pyrex filter (opaque for $\lambda < 290$ nm) limits excitation to the $^3P_1$ state, and the cold matrix photochemistry we observed here must therefore proceed through this $^3P_1$ metal excited state. Furthermore, the growth of CdH_2 using the 313 nm band pass interference filter clearly limits excitation to the $^3P_1$ Cd state. The bent triplet (H−M−H)* intermediate so formed is deactivated by collisions within the matrix cage to the linear singlet ground state metal dihydride molecule, reaction 1. It is unlikely that significant (H−M−H)* deactivation occurs by recombination of H and MH in the matrix cage as H atoms can diffuse readily in solid argon. The observed slow growth of bands due to the metal dihydride may then be attributed to the low transition probability governing the population of the $^3P_1$ excited state. Activation energy for the pulsed-laser-evaporated atom reactions is expected to arise from the excess of kinetic energy possessed by the metal atom,[49,50] although metal resonance radiation emanating from the target surface may also result in excitation of the metal atom reagent.

$$Zn(^3P_1) + H_2 \rightarrow (H{-}Zn{-}H)^* \xrightarrow{\text{matrix cage}} H{-}Zn{-}H \quad (1)$$

$$Cd(^3P_1) + H_2 \rightarrow (H{-}Cd{-}H)^* \xrightarrow{\text{matrix cage}} H{-}Cd{-}H$$

The observation that the H−Zn−D and H−Cd−D isotopic species are the primary products of the HD reactions confirms the mechanism. Weak absorptions for ZnH_2 and ZnD_2 in the HD experiment point to a small contribution from secondary reactions between H and ZnH during sample deposition. After annealing to 20−25 K, most of the H_2 escapes the matrix and little photochemical growth of ZnH_2 and CdH_2 was observed thereafter. However, photolysis before annealing produced a 2−4-fold growth of ZnH_2 and CdH_2 absorptions. Finally, it must be noted that even though decomposition of ZnH_2 and CdH_2 back to the metal atom and dihydrogen are *exothermic* processes, substantial barriers must exist for decomposition of these stable, linear molecules.

The 1849.6 and 600.0 cm^{-1} bands in the Zn/H_2 experiments grow on photolysis, as do the bands of the dihydride, but remain on annealing while those of ZnH_2 decrease. An analogous set of features was observed in the Cd/H_2 experiment at 1718.6 and 586.7 cm^{-1}. These bands are more likely to arise from a complex of the metal dihydride, possibly with H_2, than from H−Zn−Zn−H, to which they were tentatively assigned, by Xiao et al.,[8] for reasons to be discussed below. In addition, the 600 cm^{-1} band is clearly a satellite of the 630.5 cm^{-1} ZnH_2 bending mode, as analogous satellites appear at 431.7 cm^{-1} for the ZnD_2 bending mode (at 454.4 cm^{-1}) and, of more importance, at 528.9 cm^{-1} for the HZnD bending mode (at 553.4 cm^{-1}). Finally, the Zn/H_2 experiments revealed a set of bands centered at 1824.4 and 578.8 cm^{-1} which grew markedly on annealing; these are assigned to perturbed ZnH_2 where the perturbing species may be Zn atoms. Again, the observation of ZnD_2 and HZnD bending mode counterparts (at 416.2 and 511.1 cm^{-1}) upholds the view that these bands relate to a perturbed ZnH_2 motion. No analogous perturbed CdH_2 species was identified.

MH. A new feature centered at 1493.9 cm^{-1} in the zinc/hydrogen discharge and pulsed-laser experiments and shifting to 1087.5 cm^{-1} in the zinc/deuterium experiments (H/D = 1.3737) was not reported by Xiao et al.[8] This sharp band is assigned to the diatomic ZnH. We note that the same ZnH and ZnD bands were observed unshifted in HD experiments. Vibrational frequencies of 1496.5 and 1090.0 cm^{-1} have been determined for gaseous ^{64}ZnH and ^{64}ZnD, respectively, using $\nu = Y_{10} + 2Y_{20}$ and the available Dunham parameters.[51−53] The values observed for the matrix-isolated molecules are thus red-shifted by only 2.6 and 2.5 cm^{-1}, respectively, from the gas-phase values. Similar features in the cadmium experiments, observed at 1339.4 and 974.4 cm^{-1} (H/D = 1.3746), are assigned to CdH and CdD. These frequencies are also in close agreement with the gas-phase values of 1336.9 and 973.6 cm^{-1}, again calculated from the experimentally available Dunham parameters.[52,53]

Recent studies[11] of the gas-phase reaction between $Zn(^3P_1)$ and H_2 have suggested that the formation of the monohydride ZnH mainly proceeds via the decomposition of the energetically excited bent H−Zn−H insertion product, reaction 2. This reaction occurs in the gas phase during condensation and the ZnH and CdH products are trapped in the argon matrix; the reduced yield of ZnH in the separate deposition experiment with minimum reagent mixing attests to gas phase reaction 2 in the discharge region.

$$Zn(^3P_1) + H_2 \rightarrow (H{-}Zn{-}H)^* \rightarrow ZnH + H \quad (2)$$

$$Cd(^3P_1) + H_2 \rightarrow (H{-}Cd{-}H)^* \rightarrow CdH + H$$

It is noteworthy that ZnH and CdH photolyze efficiently in the present experiments under the action of light in the 290−400 nm range which can excite only the bound A and B states of ZnH and CdH.[32] Thus the observed response to photolysis is most likely due to local heating and diffusion, which allows for combination of H with ZnH or CdH. In the Zn experiment, photolysis with $\lambda > 310$ nm cannot result in the formation of ZnH_2 by reaction 1, and so the demise of ZnH by reaction with H atoms is probable and accounts for the small increase we observe in ZnH_2. The reaction between H and ZnH to give ZnH_2 is strongly exothermic; the calculated energy change is −3.4 eV at the MP2B level.

Finally, the spectra showed weak bands at 1530.5 and 1372.9 cm^{-1}, which also increased on annealing and decreased on photolysis. These are probably due to H_2 complexes with ZnH and CdH, respectively. Similar H_2 complexes with MgH and BH have been observed blue-shifted by 43 and 39 cm^{-1}, respectively.[10,54] A weak band in the Zn/H_2 system at 1540 cm^{-1}, which has a counterpart in the analogous cadmium experiment at 1379.6 cm^{-1}, is also probably due to a perturbed monohydride molecule where the perturbation may be caused by a metal atom.

M_2H. The strong band at 1657.6 cm^{-1} associated with a photosensitive ($\lambda > 290$ nm) product in the Zn/H_2 experiments and a number of weaker bands remain to be assigned. A band at 1667.5 cm^{-1} that appeared on annealing in the Zn/H_2 experiments is believed to be due to the same species that gives

rise to the 1657.6 cm^{-1} band. An analogous Cd species yields a band at 1521.0 cm^{-1}. *In addition, the hydrogen and deuterium counterparts* (Tables 3 and 4) *were unshifted in the HD experiments.* Hence, the 1657.6 cm^{-1} band is due to a species with a single H atom. Zinc concentration studies point to more metal atoms in this new species than in ZnH_2. The MP2B frequency calculations predict a Zn−H stretching frequency for the ZnZnH species approximately 170 cm^{-1} *below* the ν_3 mode of ZnH_2. We note that MP2 calculations are expected to be more approximate for open-shell systems; for example, the harmonic frequency of ZnH is predicted to be some 210 cm^{-1} above the observed matrix value. The 1657.6 cm^{-1} band coming 213 cm^{-1} *lower* than the ν_3 mode of ZnH_2 is thus in line with the MP2B frequency calculations. Accordingly, the bands at 1667.5 and 1657.6 cm^{-1} are assigned to the Zn−H stretching mode of Zn−Zn−H in different matrix environments, and the band at 1521.0 cm^{-1} to the analogous Cd species. The dimetal monohydrides are probably made by addition of a metal atom to the monohydride, a reaction which is expected to occur without activation energy.

$$Zn + ZnH \rightarrow ZnZnH \qquad (3)$$

$$Cd + CdH \rightarrow CdCdH$$

HZnZnH. The Rice group[8] observed in Zn/H_2 experiments that photolysis brought about the growth of bands at 1850.1 and 600.8 cm^{-1} and tentatively assigned these bands to Zn_2H_2. The present ab initio calculations show, however, that this identification is not correct because the antisymmetric Zn−H stretching frequency of linear H−Zn−Zn−H should fall at least 100 cm^{-1} below that of ZnH_2, while the infrared-active bending mode should be in the 300−400 cm^{-1} region. Furthermore, the weak Zn−Zn bond suggests that H−Zn−Zn−H will photolyze under the conditions of these experiments. In addition, the MP2B calculations for HZnZnD predict that, in frequency terms, the terminal Zn−H stretching mode should exceed the σ_u mode of HZnZnH by about 17 cm^{-1}, and likewise that the terminal Zn−D mode should exceed the σ_u mode of DZnZnD by about 12 cm^{-1}. The sharp, weak features at 1740.3 cm^{-1} in H_2 experiments and at 1254.9 cm^{-1} in D_2 experiments grow on annealing up to about 40 K and are destroyed on photolysis ($\lambda > 290$ nm). The H/D ratio (1.3868) is comparable to the ratio for HZnH and appropriate to HZnZnH. The new bands in the HD experiments at 1756.4 and 1267.1 cm^{-1} are 16 and 12 cm^{-1} in excess of the σ_u modes for the HZnZnH and DZnZnD isotopic species, respectively, in very good agreement with the calculated isotopic shifts. Finally, the MP2B calculations on closed-shell HZnH and HZnZnH species predict that the antisymmetric Zn−H stretching mode of the latter should occur 117 cm^{-1} below the corresponding mode of the former. In fact, the 1740.3 cm^{-1} band is observed to be 130 cm^{-1} lower, in very good agreement with this prediction. Accordingly, the weak 1740.3 cm^{-1} band is assigned to the σ_u mode of HZnZnH on the basis of the isotopic shifts and MP2B calculations. The analogous cadmium species was not detected.

The HZnZnH species is most likely formed on dimerization of the monohydride, a process calculated to be exothermic by 2.58 eV and expected to proceed spontaneously on diffusion of ZnH during sample annealing. The detection of HZnZnH and DZnZnD in the HD experiments rules out the insertion reaction of Zn_2 into HD.

$$ZnH + ZnH \rightarrow HZnZnH \qquad (4)$$

$H_2O\cdots M$. As mentioned previously, weak bands at 1587.4 and 1585.3 cm^{-1} are in agreement with the previous assignment to $H_2O\cdots Zn$.[43] Analogous bands at 1580.7 and 1572.4 cm^{-1} in Cd/H_2 experiments grow on annealing and decrease on photolysis. The Cd/D_2 counterparts at 1168.4 and 1161.5 cm^{-1} exhibit similar behavior and define H/D ratios of 1.3529 and 1.3538 which are appropriate for an O−H vibration of the analogous $H_2O\cdots Cd$ complex. We note that Cd perturbs ν_2 of water slightly more than does zinc.

HMOH. Several transition-metal species of the type HMOH have been prepared by photolysis of metal/water matrix samples.[43] These products are characterised by M−H and M−O stretching modes and by a low-frequency bending mode. The molecule HCuOH, most nearly like HZnOH, exhibits such bands at 1911, 616, and 668 cm^{-1}, respectively. Bands assigned here to HZnOH and HCdOH, formed from trace water impurities present in the matrix, grow on photolysis at the expense of the bands due to $H_2O\cdots M$ complexes but increase little when water is added on purpose.[55]

Charged Species. Exposure of M/H_2 mixtures (M = Zn or Cd) to the resonance radiation from the argon/metal/hydrogen discharge invites consideration of the possible intervention of charged species.[49] The band at 905 cm^{-1} could in fact be due to the Ar_nH^+ species, but the absence of an Ar_nD^+ counterpart and the stability to photolysis imply otherwise. The fundamental of gaseous ZnH^+ at 1838 cm^{-1} [30] is expected to be red-shifted by the matrix. The weak band at 1782.2 cm^{-1} exhibits an appropriate H/D ratio (1.3875) for tentative assignment to ZnH^+; this band was observed to decay on photolysis, as expected for a positive ion isolated in a matrix containing counterions.[56]

Conclusions

The microwave discharge-powered reactive resonance lamp is an effective method for activating Zn and Cd atoms for reaction with H_2. Similar products are generated by thermal evaporation/photolysis[8] and pulsed-laser evaporation and reaction. Ab initio calculations at the MP2B level produce a trend in stretching frequencies for the major product molecules HZnH, HZnZnH, ZnZnH, and ZnH and isotopic frequencies which are important for the identification of these molecules on the basis of the experimental spectra. The dihydride ZnH_2 is suggested by gas phase studies[11] to be the insertion intermediate in the reaction of excited zinc with dihydrogen; the ZnH_2 molecule has been formed, deactivated and trapped in solid argon. Pyrex-filtered photolysis studies show that ^3P excited metal atoms react with H_2 in the matrix to form the metal dihydride molecules. The dizinc molecules ZnZnH and HZnZnH are shown to be photosensitive, as expected for species with weak metal−metal bonds.

Acknowledgment. The authors thank the EPSCR (formerly SERC) for support of this research, including a research assistantship for T.M.G. L.A. was a sesquicentennial associate of the University of Virginia and a Senior Fulbright Scholar while a Senior Academic Visitor at the University of Oxford. The pulsed-laser experiments were supported by NSF(US) Grant CHE 91−22556. The computations were carried out on the Convex, Cray, and IBM machines at the Center for Scientific Computing, Espoo, Finland. A visit of P.P. to Oxford was supported by REHE/ESF. N.R. is supported by The Academy of Finland.

References and Notes

(1) Barbaras, G. D.; Dillard, C.; Finholt, A. E.; Wartik, T.; Wilzbach, K. E.; Schlesinger, H. I. *J. Am. Chem. Soc.* **1951**, *73*, 4585.
(2) Ashby, E. C.; Watkins, J. J. *Inorg. Synth.* **1977**, *17*, 6.
(3) Wiberg, E.; Henle, W. *Z. Naturforsch.* **1951**, *6b*, 461.

(4) Smith, G. S.; Johnson, Q. C.; Smith, D. K.; Cox, D. E.; Snyder, R. L.; Zhou, R.-S.; Zalkin, A. *Solid State Commun.* **1988**, *67*, 491.
(5) Zachariasen, W. H.; Holley, C. E., Jr.; Stamper, J. F., Jr. *Acta Crystallogr.* **1963**, *16*, 352.
(6) Turley, J. W.; Rinn, H. W. *Inorg. Chem.* **1969**, *8*, 18.
(7) McCaffrey, J. G.; Parnis, J. M.; Ozin, G. A.; Breckenridge, W. H. *J. Phys. Chem.* **1985**, *89*, 4945.
(8) Xiao, Z. L.; Hauge, R. H.; Margrave, J. L. *High Temp. Sci.* **1991**, *31*, 59.
(9) Tague, T. J., Jr.; Andrews, L. *J. Am. Chem. Soc.* **1993**, *115*, 12111.
(10) Tague, T. J., Jr.; Andrews, L. *J. Phys. Chem.* **1994**, *98*, 8611.
(11) Breckenridge, W. H.; Wang, J.-H. *J. Chem. Phys.* **1987**, *87*, 2630.
(12) Simons, G.; Talaty, E. R. *J. Chem. Phys.* **1977**, *66*, 2457.
(13) Pyykko, P. *J. Chem. Soc., Faraday Trans. 2* **1979**, *75*, 1256.
(14) Tyrrell, J.; Youakim, A. *J. Phys. Chem.* **1980**, *84*, 3568.
(15) Kaupp, M.; Stoll, H.; Preuss, H.; Kaim, W.; Stahl, T.; van Koten, G.; Wissing, E.; Smeets, W. J. J.; Spek, A. L. *J. Am. Chem. Soc.* **1991**, *113*, 5606.
(16) Kaupp, M.; von Schnering, H. G. *Inorg. Chem.* **1994**, *33*, 2555, 4179.
(17) Dolg, M.; Küchle, W.; Stoll, H.; Preuss, H.; Schwerdtfeger, P. *Mol. Phys.***1991**, *74*, 1265.
(18) Schwerdtfeger, P.; Heath, G. A.; Dolg, M.; Bennett, M. A. *J. Am. Chem. Soc.* **1992**, *114*, 7518.
(19) Schwerdtfeger, P.; Boyd, P. D. W.; Brienne, S.; McFeaters, J. S.; Dolg, M.; Liao, M.-S.; Schwarz, W. H. E. *Inorg. Chim. Acta* **1993**, *213*, 233.
(20) Brabson, G. D.; Mielke, Z.; Andrews, L. *J. Phys. Chem.* **1991**, *95*, 79. Brabson, G. D.; Andrews, L. *J. Phys. Chem.* **1992**, *96*, 9172.
(21) Hawkins, M.; Downs, A. J. *J. Phys. Chem.* **1984**, *88*, 1527.
(22) Burkholder, T. R.; Andrews, L. *J. Chem. Phys.* **1991**, *95*, 8697.
(23) Hassanzadeh, P.; Andrews, L. *J. Phys. Chem.* **1992**, *96*, 9177.
(24) *Gaussian 92, Revision E. 2;* Frisch, M. J.; Trucks, G. W.; Head-Gordon, M.; Gill, P. M. W.; Wong, M. W.; Foresman, J. B.; Johnson, B. G.; Schlegel, H. B.; Robb, M. A.; Replogle, E. S.; Gomperts, R.; Andres, J. L.; Raghavachari, K.; Binkly, J. S.; Gonzalez, C.; Martin, R. L.; Fox, D. J.; Defrees, D. J.; Baker, J.; Stewart, J. J. P.; Pople, J. A. Gaussian, Inc.: Pittsburgh PA, 1992.
(25) Sundius, T. *MOLVIB: A Program for Harmonic Force Field Calculations;* QCPE program No. 604, 1991. Sundius, T. *J. Mol. Struct.* **1990**, *218*, 321.
(26) Dolg, M.; Wedig, U.; Stoll, H.; Preuss, H. *J. Chem. Phys.* **1987**, *86*, 866.
(27) Andrae, D.; Häussermann, U.; Dolg, M.; Stoll, H.; Preuss, H. *Theor. Chim. Acta* **1990**, *77*, 123.
(28) Dunning, T. H., Jr.; Hay, P. J. *Mod. Theor. Chem.* **1977**, *3*, 1.
(29) Dunning, T. H., Jr. *J. Chem. Phys.* **1971**, *55*, 3958.
(30) Huzinaga, S. *J. Chem. Phys.* **1965**, *42*, 1293.
(31) Häussermann, U.; Dolg, M.; Stoll, H.; Preuss, H.; Schwerdtfeger, P.; Pitzer, R. M. *Mol. Phys.* **1993**, *78*, 1211.
(32) Huber, K. P.; Herzberg, G. *Molecular Spectra and Molecular Structure. IV. Constants of Diatomic Molecules;* Van Nostrand Reinhold: New York, 1979.
(33) Redington, R. L.; Milligan, D. E. *J. Chem. Phys.* **1963**, *39*, 1276.
(34) DiLella, D. P.; Tevault, D. E. *Chem. Phys. Lett.* **1986**, *126*, 38.
(35) Nelander, B. *J. Phys. Chem.* **1985**, *89*, 827.
(36) Milligan, D. E.; Jacox, M. E. *J. Chem. Phys.* **1971**, *54*, 927.
(37) Davis, S. R.; Andrews, L. *J. Chem. Phys.* **1987**, *86*, 3765.
(38) Andrews, L.; Johnson, G. L.; Kelsall, B. J. *J. Chem. Phys.* **1982**, *76*, 5767.
(39) Andrews, L.; Johnson, G. L.; Kelsall, B. J. *J. Phys. Chem.* **1982**, *86*, 3374.
(40) Anderson, J. S.; Ogden, J. S. *J. Chem. Phys.* **1969**, *51*, 4189.
(41) Hacaloglu, J.; Suzer, S.; Andrews, L. *J. Phys. Chem.* **1990**, *94*, 1759.
(42) Smith, D. W.; Andrews, L. *J. Chem. Phys.* **1974**, *60*, 81.
(43) Kauffman, J. W.; Hauge, R. H.; Margrave, J. L. *J. Phys. Chem.* **1985**, *89*, 3541.
(44) Legay-Sommaire, N.; Legay, F. *Chem. Phys. Lett.* **1993**, *207*, 123.
(45) Chong, D. P.; Langhoff, S. R.; Bauschlicher, C. W., Jr.; Walch, S. P.; Partridge, H. *J. Chem. Phys.* **1986**, *85*, 2850.
(46) Jamorski, Ch.; Dargelos, A.; Teichteil, Ch.; Daudey, J. P. *J. Chem. Phys.* **1994**, *100*, 917.
(47) Ault, B. S.; Andrews, L. *J. Mol. Spectrosc.* **1977**, *65*, 102.
(48) Wallace, I.; Funk, D. J.; Kemp, J. G.; Breckenridge, W. H. *J. Chem. Phys.* **1992**, *97*, 3135.
(49) Andrews, L.; Burkholder, T. R.; Yustein, J. T. *J. Phys. Chem.* **1992**, *96*, 10182.
(50) Salzberg, A. P.; Santiago, D. I.; Asmar, F.; Sandoval, D. N.; Weiner, B. R. *Chem. Phys. Lett.* **1991**, *180*, 161.
(51) Herzberg, G. *Molecular Spectra and Molecular Structure. I. Spectra of Diatomic Molecules,* Van Nostrand: Princeton, NJ, 1950.
(52) Urban, R.-D.; Magg, U.; Birk, H.; Jones, H. *J. Chem. Phys.* **1990**, *92*, 14.
(53) Birk, H.; Urban, R.-D.; Polomsky, P.; Jones, H. *J. Chem. Phys.* **1991**, *94*, 5435.
(54) Tague, T. J., Jr.; Andrews, L. *J. Am. Chem. Soc.* **1994**, *116*, 4970.
(55) Greene, T. M.; Andrews, L.; Downs A. J., unpublished results.
(56) Andrews, L. *Annu. Rev. Phys. Chem.* **1979**, *30*, 79.

JP942926X